



HAL
open science

Structural and rheological analysis of nickel enriched peraluminous glasses

Erik Hansen, Damien Perret, Isabelle Giboire, Sylvain Mure, Christophe Rapin

► **To cite this version:**

Erik Hansen, Damien Perret, Isabelle Giboire, Sylvain Mure, Christophe Rapin. Structural and rheological analysis of nickel enriched peraluminous glasses. *Journal of Non-Crystalline Solids*, 2021, pp.DOI: 10.1016/j.nocx.2021.100069. 10.1016/j.nocx.2021.100069 . cea-03442400

HAL Id: cea-03442400

<https://cea.hal.science/cea-03442400>

Submitted on 23 Nov 2021

HAL is a multi-disciplinary open access archive for the deposit and dissemination of scientific research documents, whether they are published or not. The documents may come from teaching and research institutions in France or abroad, or from public or private research centers.

L'archive ouverte pluridisciplinaire **HAL**, est destinée au dépôt et à la diffusion de documents scientifiques de niveau recherche, publiés ou non, émanant des établissements d'enseignement et de recherche français ou étrangers, des laboratoires publics ou privés.



Distributed under a Creative Commons Attribution - NonCommercial - NoDerivatives 4.0 International License

Structural and rheological analysis of nickel enriched peraluminous glasses

E. Hansen ^a, D. Perret ^{a*}, I. Bardez-Giboire ^a, S. Mure ^a, C. Rapin ^b

^a CEA, DES, ISEC, DE2D, Univ Montpellier, Marcoule, France

^b Institut Jean Lamour, Nancy, France

* Corresponding author.

Email address : damien.perret@cea.fr

Full postal address: CEA Marcoule, ISEC/D2ED/SEVT/LDMC, BP 17171, F-30207 Bagnols-sur-Cèze, France

ABSTRACT

This study describes the role of nickel oxide (NiO) in peraluminous glass. Peraluminous glass is defined by an excess of aluminium ions (Al^{3+}) compared to modifier elements such as Na^+ , Li^+ or Ca^{2+} ions. The study investigates the effect NiO incorporation on peraluminous glass homogeneity and process ability. Quenched NiO-containing glass showed an incorporation limit greater than 12 wt% NiO (13.8 mol%), while slowly cooled glass showed a limit of 5 wt% NiO (5.8 mol%). Nickel oxide is also found to have a fluidifying effect on peraluminous glasses. When the nickel oxide content is above its incorporation limit, the resulting crystals were found to have a significant effect on glass rheological properties. Finally, hypotheses are proposed as to the structural role of Ni in peraluminous glass based on the experimental results obtained.

Keywords:

Peraluminous glass, incorporation limit, crystallization, viscosity, nickel oxide

1. Introduction

Present mostly under the stable form Ni^{2+} without any other valences, nickel is a reliable colouring agent for borosilicate glasses. Depending on the glass composition, Ni^{2+} can adopt several coordinations ^[1-5]: tetrahedral $Ni^{2+}[4]$, trigonal bipyramid $Ni^{2+}[5]$, square pyramid $Ni^{2+}[5]$ and octahedral $Ni^{2+}[6]$.

Ni^{2+} coordination has been studied by UV-Visible spectroscopy in silicates ^[1, 2, 5], borates ^[6], aluminosilicates ^[1, 2, 3, 7] and borosilicates ^[8]. Ni^{2+} exhibits specific colours depending on the coordination it takes: pink for tetrahedral $Ni^{2+}[4]$, or green-blue for $Ni^{2+}[6]$ ^[8], while glasses containing $Ni^{2+}[5]$ have colours varying from yellow-brown or brown to red-pink. In the latter glasses, $Ni^{2+}[5]$ was associated with $Ni^{2+}[4]$ and a mix of $Ni^{2+}[4]$ and $Ni^{2+}[6]$ respectively ^[3]. If the role of nickel is fairly well understood in peralkaline glass, to our knowledge its role in peraluminous glass has not yet been investigated. Peraluminous glasses have already been proven to be able to incorporate up to 25 wt% of rare earths, making them potentially interesting for hosting nuclear waste ^[9-11]. Peraluminous glass is characterized by the presence of high amounts of alumina and lower amounts of modifier oxides like sodium and calcium oxides. A glass composition domain is traditionally called “peralkaline” when the Rp ratio > 0.50 and “peraluminous” when the Rp ratio < 0.50. The Rp ratio is defined by equation (1).

$$Rp = \frac{\text{modifiers}}{Al_2O_3 + \text{modifiers}} \quad (1)$$

Firstly, this work focuses on determining NiO incorporation limit in peraluminous glass, considering the thermal history of the glass. The nickel coordination in these samples was also studied. Secondly, the effect of NiO on glass viscosity was investigated. From these results, hypotheses as to the role and environment of nickel in peraluminous glass are discussed.

2. Experimental

2.1. Glass compositions

Peraluminous glasses are known to remain highly viscous even at high temperatures. One composition of peraluminous glass studied by Piovesan et al. ^[11] was selected to serve as a reference for this work. This reference composition was chosen among 21 glass compositions from the design of experiments conducted by Piovesan et al. Several criteria were considered in selecting this composition, for example melt viscosity and the absence of crystallization. From this reference composition named EH BASE 0, 10 glass compositions were studied while increasing the NiO content from 0.5 wt% to 15 wt% (Table 1).

2.2. Thermal scenario

The glass samples were obtained either by a cast of the melt (as-quenched glass), or after a slow cooling of the glass. As-quenched glasses, named “CP” (in French “Coulé sur Plaque”), were obtained using a double fusion followed by a quench of the melt on a steel plate. Slowly-cooled glasses, named “RLT” (in French “Refroidi Lentement en Température”), were obtained by a slow cooling at 1°C per minute from 1350°C down to room temperature.

2.3. Experimental methods

Homogeneous mixtures of batches were obtained by mixing oxide precursors (SiO₂, CaO, Li₂CO₃, La₂O₃, Al₂O₃, H₃BO₃, Na₂CO₃, NiO) as powders. Batches were preheated in Pt-Rh crucibles for decarbonisation at 500 °C for 3 hours, then melted at 1350 °C for a further 3 hours. In order to avoid unmelted particles, the glass samples were made using double elaboration process. Samples were first cast onto steel plates, then milled down into powder using a WC mill with WC marbles. This glass powder was heated again in the same Pt-Rh crucible at 1350°C for 2h. The melt was then quenched on steel-plates, leading to CP glass samples. About 40g of glass were taken and melted for 45 minutes at 1350°C in a Pt-Au crucible and then slowly cooled at 1°C per minute until room temperature was reached, giving the RLT glass samples.

The amorphous or crystalline nature of quenched and slowly-cooled glass samples was determined with X-Ray diffraction analysis (XRD), optical microscopy and Scanning Electron Microscopy (SEM). Where crystals were present, their composition was extrapolated from EDS (Energy Dispersive X-Ray Spectroscopy) measurements and confronted to XRD results.

XRD measurements were performed with a Bragg-Brentano diffractometer (Panalytical X'Pert MPD Pro). The samples were crushed to a powder finer than 100 microns in a WC mill and loaded in steel holders. Data were collected in the 2 θ range = 10-90°. XRD results were peak-matched to crystal phases detailed in the Joint Committee on Powder Diffraction Standards (JCPDS). The PDF4+ database and EVA version 5.0 software were used.

Optical microscopy was performed on a ZEISS Axio Imager M2 microscope with an Axiocam 305 camera and EC Epiplan-Neofluar (x1.25, x5, x20, x50 and x100 HD DIC M27) objectives. The samples were mirror polished. The images were collected and analysed with the Zen2Core v2.5 software.

Scanning Electron Microscopy observations of polished and metallized samples were performed on a SEM ZEISS SUPRA 55 at 15 kV. EDS analyses (Energy Dispersive X-ray Spectroscopy) were performed to obtain quantitative data of the glass and crystalline phase compositions. Large numbers of crystal compositions were collected through these EDS measurements. EDS data were confronted to XRD patterns in order to obtain reliable crystalline phase compositions. The ESPRIT 2.0 software was used for data collection and processing. Additional quantitative data were collected by microprobe

analysis performed on a CAMECA SX FIVE FE TACTIS (12 keV, 10nA) coupled with WDS (wavelength dispersive X-ray spectroscopy) analysis.

UV-Visible spectra were collected using a CARY50SCAN spectrophotometer in the range 200-1100 nm. The software used for data processing was CARY WINUV and UV-Visible spectra were deconvoluted using the OriginPro2015 software. Due to the high absorbance of nickel in this range of wavelengths, analysis was limited to glasses containing less than 12 wt% NiO and very thin samples were prepared (down to 100 microns).

Viscosity measurements were performed on a LAMY RM300i stress-imposed rheometer placed above a vertical tubular furnace able to heat up to 1500°C. Viscosity measurements were carried out on the CP glass samples. The samples were first melted at 1200°C in a Pt-Rh crucible (crucible radius $R_e = 13,5$ mm) and then placed in the furnace centre. The temperature difference measured between the top and the bottom of the melt was lower than 2°C. A platinum cylinder suspended from the viscosimeter was immersed and rotated in the melt. Rheological measurements were carried out in a steady state regime by imposing successive shear stress values, from 1 to 500 Pa, for 60 s. Angular velocity measurements were averaged during the last 10 s when the signal was stationary. For this study, the rheological behaviours of four samples were determined at temperatures ranging from 1100°C to 1500°C. Viscosity values were measured until the Newtonian behaviour loss was reached. Experimental relative error on viscosity values has been estimated as 10% from historical data.

The glass transition temperature (T_g) was determined by Differential Thermal Analysis (DTA). Glass powder amounts of about 50 mg were heated in alumina crucibles. A Setsys Evolution DTA furnace from Setaram was used to perform the DTA measurements, coupled with the Setsys-1750Cs Evol.-TG-DTA1600°C program. T_g was extracted from DTA data using the Setaram Calisto Processing software. The T_g standard error estimation is 6°C.

Oxide wt%	EH BASE-0	EH Ni-0.5	EH Ni-1	EH Ni-5	EH Ni-6	EH Ni-6.5	EH Ni-7.5	EH Ni-10	EH Ni-12	EH Ni-13.5	EH Ni-15
SiO ₂	30.96	30.81	30.65	29.42	29,11	28,95	28,64	27,87	27,25	26,78	26,32
CaO	2.95	2.94	2.92	2.80	2,77	2,76	2,73	2,65	2,60	2,55	2,51
Li ₂ O	0.59	0.59	0.58	0.56	0,55	0,55	0,55	0,53	0,52	0,51	0,50
La ₂ O ₃	26.11	25.98	25.85	24.81	24,55	24,42	24,16	23,50	22,98	22,59	22,20
Al ₂ O ₃	20.44	20.33	20.23	19.41	19,21	19,11	18,90	18,39	17,98	17,68	17,37
B ₂ O ₃	16.11	16.03	15.95	15.30	15,14	15,06	14,90	14,50	14,17	13,93	13,69
Na ₂ O	2.84	2.83	2.81	2.70	2,67	2,66	2,63	2,56	2,50	2,46	2,41
NiO	-	0.50	1.00	5.00	6.00	6.50	7.50	10.00	12.00	13.50	15.00
Total	100.00	100.00	100.00	100.00	100.00	100.00	100.00	100.00	100.00	100.00	100.00

Table 1: Glass sample compositions (wt%)

3. Results

3.1. Incorporation limits

The incorporation limits of NiO in peraluminous glass were determined with respect to the thermal history of the glass. Therefore, incorporation limits are given for both as-quenched glasses (CP) cast at 1350°C and for slowly cooled glasses (RLT). The results are summarized in Table 2. SEM images showing the appearance of the first crystals are given in Figure 10 in the Appendix.

Glass name	EH BASE-0	EH Ni-0.5	EH Ni-1	EH Ni-5	EH Ni-6	EH Ni-6.5	EH Ni-7.5	EH Ni-10	EH Ni-12	EH Ni-13.5	EH Ni-15
NiO wt%	0	0.5	1.0	5.0	6.0	6.5	7.5	10.0	12.0	13.5	15.0
NiO mol%	0	0.6	1.2	5.8	6.9	7.5	8.7	11.5	13.8	15.4	17.1
CP Glass	no crystal	no crystal	no crystal	no crystal	no crystal	Few crystals (surface)	Few crystals (surface)				
RLT Glass	no crystal	no crystal	no crystal	no crystal	Few crystals (surface)	Few crystals (surface)	Few crystals (surface)	Crystals (bulk)			Crystals (bulk)

Table 2 : Determination (SEM and optical microscopy) of the presence of crystals in as-quenched (CP) and slowly-cooled (RLT) glass samples. As-quenched samples were cast at 1350°C.

3.2. Crystallization behaviour

3.2.1. As-quenched glasses (CP)

Crystalline phases identification was carried out in as-quenched glasses with compositions above the NiO incorporation limit. The glass samples of interest were EH Ni-13.5 CP and EH Ni-15 CP, containing 13.5 wt% and 15 wt% NiO, respectively. Below 13.5 wt% NiO, as-quenched samples did not show any crystals. The EH Ni-13.5 CP and EH Ni-15 CP glasses showed the same crystals: a primary phase made of NiO crystals, and a secondary phase made of a Ni-containing spinel crystals. The NiO crystals were identified under both SEM/EDS analysis (Figure 10 in Appendix) and XRD. XRD traces were peak-matched to the NiO phase detailed in the JCPDS card n°00-047-1049 (Figure 11). The NiO crystal size depended on the initial NiO content: about 2µm and 10µm in glasses containing 13.5 and 15 wt% NiO, respectively.

Small crystals appeared in the vicinity of NiO crystals, as observed on the SEM images (Figure 10). These crystals are darker than the NiO crystals, indicating the presence of elements with lower weight than Ni. The XRD peaks are well matched to both JCPDS cards n°04-005-6872 and n°00-015-0255 associated with NiAl₂O₄ and Ni₂SiO₄ spinel phases, respectively. The spinel crystal amount and size were too small in these as-quenched samples for a more accurate identification at this stage.

3.2.2. Slowly cooled glasses (RLT)

Slowly cooled glasses were amorphous up to 5 wt% NiO and did not show any crystals. Above 6 wt% NiO, the samples contained several types of crystals. The first type is a phase containing Ni, Al, O, and at least one other element that was not detectable under SEM/EDS. The missing element was boron, and the phase was identified by XRD as dinickelaluminoborate Ni₂Al(BO₃)O₂ (JCPDS card n°04-009-4981, as seen in Figure 14 and Figure 15). Ni₂Al(BO₃)O₂ stoichiometry was also confirmed by microprobe/WDS measurements (Figure 16 and Figure 17), able to quantify boron. Finally, the Al and Ni contents in these crystals measured by EDS analysis were close to those calculated from Ni₂Al(BO₃)O₂ stoichiometry (Figure 18). The Ni₂Al(BO₃)O₂ crystals had a dendritic pattern, with sizes from a few microns up to 1500 µm for the sample with the highest NiO content (15 wt%).

The second type of crystals was a NiAl₂O₄ spinel phase. These crystals appeared as small squares near the surface of the glass and as large patterns (about 100 to 200 µm) deeper in the glass bulk. For bigger spinel crystals, a local enrichment in silicon can be seen at the tip of the crystals. Quantitative analysis by SEM-EDS showed that the spinel phase was made of both NiAl₂O₄ and Ni₂SiO₄ in these areas. The NiAl₂O₄:Ni₂SiO₄ molar ratio goes from around 1:1 at the tip of the crystals to 1:0 (NiAl₂O₄

alone) far from the crystal/glass matrix interface. The SEM images and EDS analyses are given in Figure 18 and Figure 19. The spinel crystals are detectable by XRD as shown in Figure 14 and Figure 15 but peak indexation using JCPDS cards n°04-005-6872 and 00-015-0255 for NiAl₂O₄ and Ni₂SiO₄ respectively could not distinguish the two phases due to very close lattice systems. Further investigation using a different JCPDS database for peak indexation might provide additional information, but this was outside the scope of this work. However, a hypothesis is suggested that this spinel phase may be a spinel solid solution, as discussed later in the paper. Spinel solid solutions are not so common but have already been described in the literature ^[12, 13].

At 15 wt% NiO, two additional crystalline phases can be observed: the primary NiO phase, and a new phase rich in lanthanum. The size of this La-containing phase did not exceed 1 μm. The stoichiometry of this phase could not be determined by XRD, by SEM-EDS, or by microprobe analysis, but a possible origin can be explained, as will be discussed later.

A summary of the crystalline phases observed in slowly cooled samples is provided in Table 3.

Glass	EH Ni-6 RLT	EH Ni-6.5 RLT	EH Ni-7.5 RLT	EH Ni-10 RLT	EH Ni-15 RLT
XRD analysis	No peak detected	No peak detected	No peak detected	Ni ₂ Al(BO ₃)O ₂ NiAl ₂ O ₄ - Ni ₂ SiO ₄	Ni ₂ Al(BO ₃)O ₂ NiAl ₂ O ₄ - Ni ₂ SiO ₄ NiO
SEM/EDS analysis	Ni ₂ Al(BO ₃)O ₂ NiAl ₂ O ₄	Ni ₂ Al(BO ₃)O ₂ NiAl ₂ O ₄	Ni ₂ Al(BO ₃)O ₂ NiAl ₂ O ₄ -Ni ₂ SiO ₄	Ni ₂ Al(BO ₃)O ₂ NiAl ₂ O ₄ -Ni ₂ SiO ₄	Ni ₂ Al(BO ₃)O ₂ NiAl ₂ O ₄ -Ni ₂ SiO ₄ NiO La-containing phase

Table 3: Crystalline phases in slowly cooled (RLT) glass samples

3.3. Determination of nickel valence and coordination

UV-visible spectroscopy measurements were carried out in order to determine the nickel valence and coordination in the peraluminous glasses investigated here. The glass thermal history was taken into account by comparing as-quenched and slowly-cooled samples. The evolution of nickel coordination when the NiO content increased in the glass was also considered. The sample colours were yellow brown to dark brown depending on NiO content and sample thickness, as seen in Figure 1.

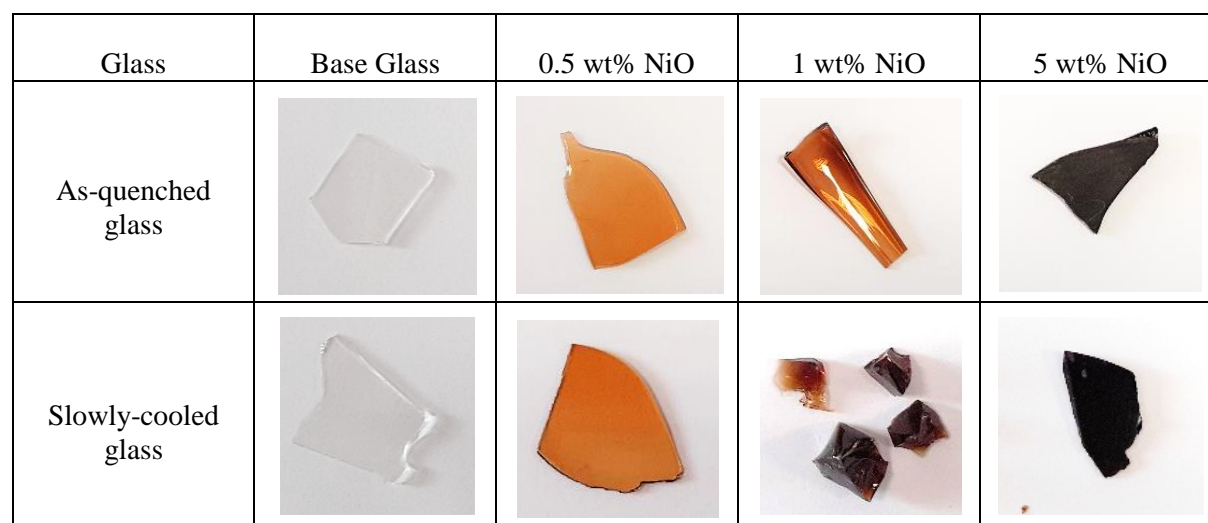


Figure 1: Colours of peraluminous glass samples containing NiO

After deconvolution, the UV-visible spectra showed absorption bands around 429 nm, 473 nm, 533 nm and 606 nm (Figure 2). These bands correspond to the following nickel structures: square pyramid $Ni^{2+}[5]$ at 429 nm, trigonal bipyramid $Ni^{2+}[5]$ at 473 nm, and tetrahedral $Ni^{2+}[4]$ at 533 nm and 606 nm [1-6, 14]. The evolution of UV-visible absorption spectra with glass thermal history show that the bands at 533 nm and 606 nm are more intense for slowly cooled (RLT) glass samples than for the as-quenched (CP) samples (Figure 3). The peak at 429 nm is, inversely, more intense for as-quenched glass samples. This would indicate that nickel coordination tends to evolve from a five-fold to a four-fold coordination during a slow cooling of the glass, as will be discussed later. The nickel coordination also tended to shift towards a four-fold coordination when the amount of NiO added to the peraluminous glass increased (Figure 4).

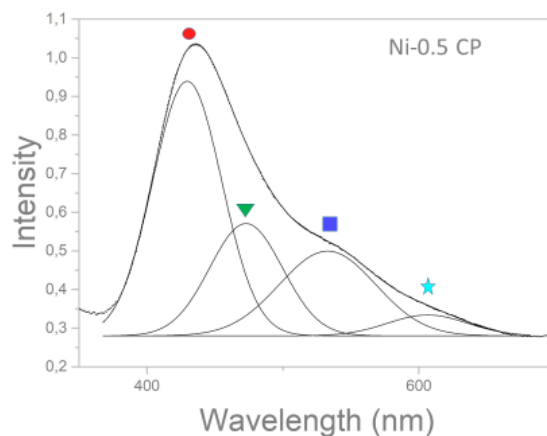


Figure 2: Deconvoluted EH Ni-0.5 CP UV-visible absorption spectra : ● 429 ±1 nm $Ni^{2+}[5]$ Square Pyramid (SP), ▼ 473 ±2 nm $Ni^{2+}[5]$ Trigonal Base Pyramid (TBP), ■ 533 ± 4 nm and * 606 ± 6 nm $Ni^{2+}[4]$ Tetrahedral (Td)

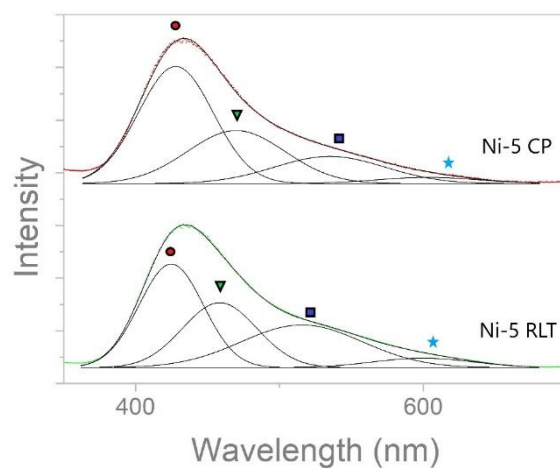


Figure 3: Comparison of the UV-Visible spectra of EH Ni-5 CP and EH Ni-5 RLT : ● $Ni^{2+}[5]$ SP, ▼ $Ni^{2+}[5]$ TBP, ■ and * $Ni^{2+}[4]$ Td

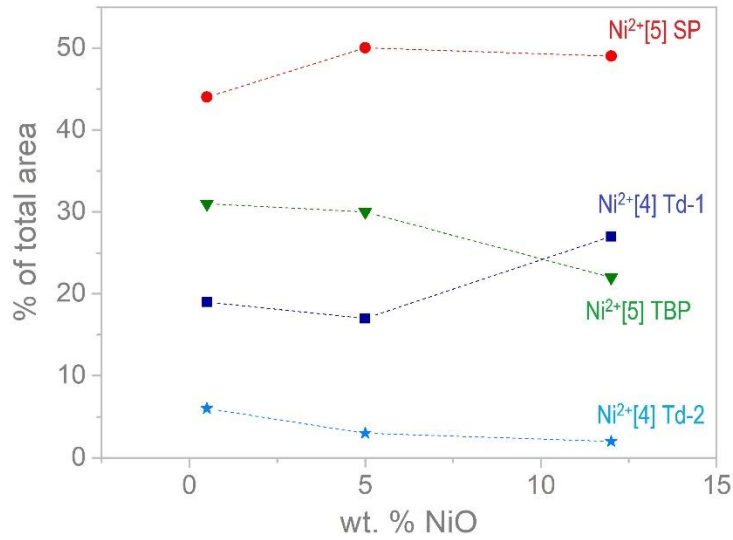


Figure 4: Evolution of CP glass coordination with NiO amount : ● Ni²⁺[5] SP, ▼ Ni²⁺[5] TBP, ■ and * Ni²⁺[4] Td

3.4. Rheological properties

The glass viscosities as a function of both temperature and NiO content are reported in Figure 5 and Figure 6, respectively. The plotted viscosity values are those for which a Newtonian behaviour was observed, meaning that glass viscosity did not depend on the shear rate. The viscosity relationship with temperature follows a classical VTF (Vogel, Tammann, Fulcher) curve, and NiO addition resulted in a strong modification of the glass viscosity. Viscosity values for the EH BASE-0 sample (reference glass) were taken from Piovesan ^[11] and were obtained using the same experimental device and protocol.

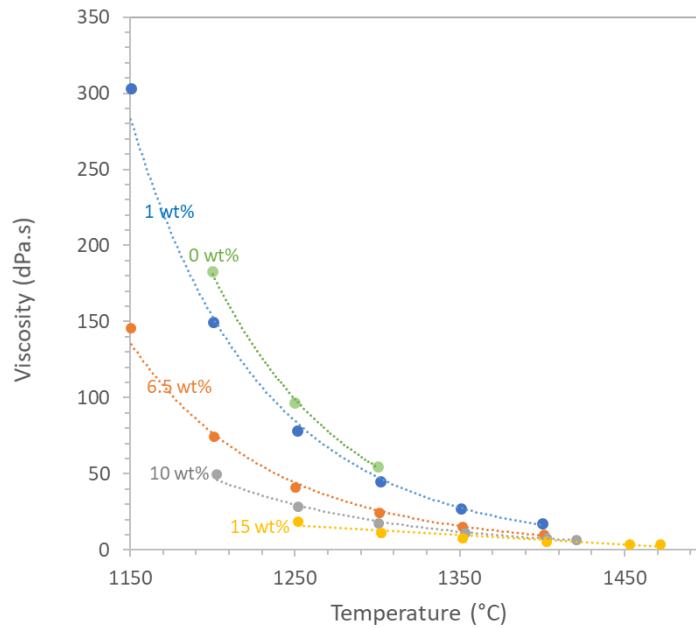


Figure 5: Glass viscosity evolution with temperature for various NiO contents

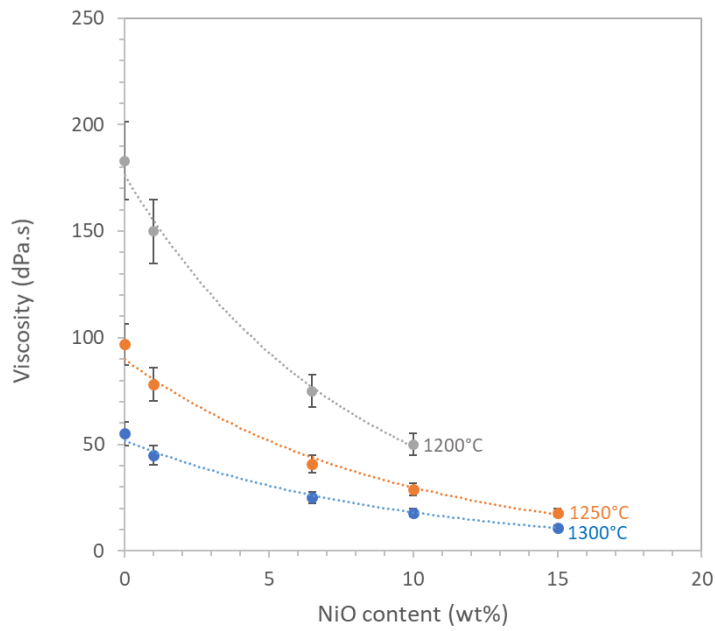


Figure 6: Glass viscosity evolution with NiO content at 1200°C, 1250°C and 1300°C

In the case where high amounts of crystals were present in the glass melt, the glass viscosity became dependant on the shear rate and the rheological behaviour is said to be non-Newtonian. A non-Newtonian behaviour can easily be observed experimentally, as shown in Figure 21 in Appendix. The temperature at which the melt became non-Newtonian was worth investigating because it indicates a situation where crystals are present at a given temperature in the melt. This temperature depends on the NiO content, as shown on Figure 7.

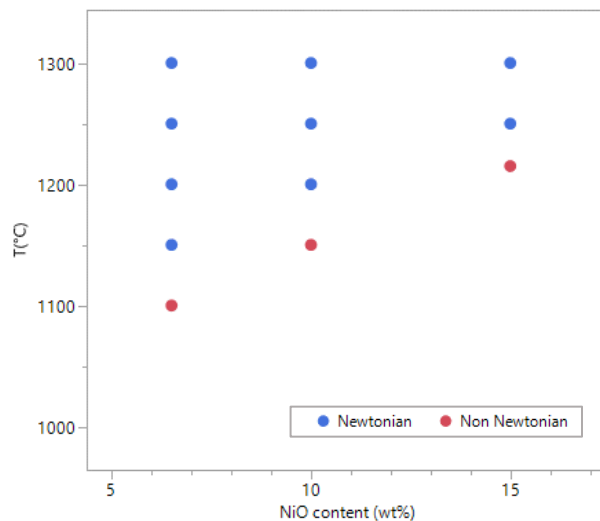


Figure 7: Rheological behaviour of the glass melt as a function of temperature and the NiO content

3.5. Glass transition temperature (T_g)

The glass transition temperature (T_g) of the peraluminous glass samples were measured by DTA as a function of NiO content. It was found that NiO addition up to 15 wt% did not lead to a significant change of T_g for either as-quenched or slowly-cooled glass samples, taking into account the experimental error, as shown in Figure 8. This result gives useful information on the role of NiO in the peraluminous silica network, as will be discussed later.

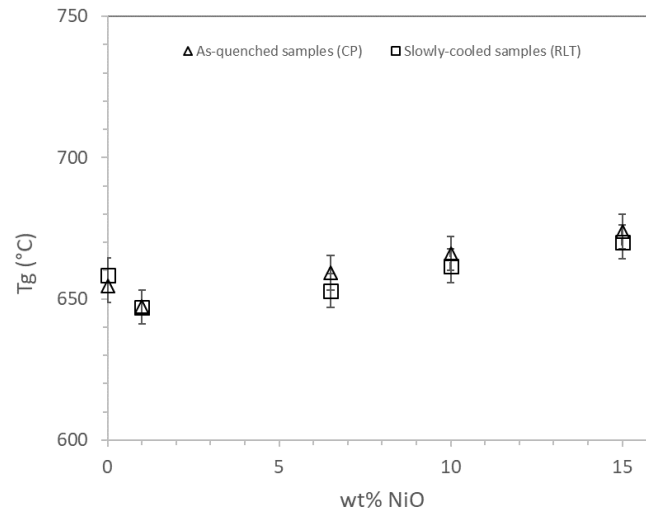


Figure 8: Glass transition temperature evolution with NiO content, for as-quenched (CP) and slowly-cooled (RLT) glass samples

4. Discussion

4.1. NiO incorporation limit

The NiO incorporation limit was determined to be between 12 wt% and 13.5 wt% NiO for as-quenched glass elaborated at 1350°C, and between 5 and 6 wt% NiO for slowly-cooled glass. The relationship between the incorporation limit and the cooling rate comes from the crystallization kinetics and the glass formation theory [15, 16]. Even when the crystalline state is thermodynamically stable, amorphous state stability is associated with atom mobility in the glass melt. In viscous liquids, molecular transport may not occur within a reasonable time scale, explaining why the presence of crystals in the glass after cooling depended on both the glass composition and the cooling rate. In this work, as-quenched glass containing up to 12 wt% NiO, even though oversaturated in NiO during cooling in the low temperatures ranges, did not lead to the formation of crystals, due to the very fast cooling rate of the glass. But when the glass was slowly cooled from 1350°C, molecular transport could occur and thus enable NiO crystallization.

Hypothetically, it was first considered that the NiO crystals observed after cooling could be NiO insoluble particles initially present at the glass melt elaboration step. This hypothesis was rejected after investigating the location of NiO crystals in the as-quenched samples, exclusively located at the glass surface but not in the bulk. These results are typical of heterogeneous nucleation, indicating a dissolution-recrystallization mechanism. In order to reinforce this assumption, a batch of the EH Ni-15 glass was cast into water in order to obtain a faster cooling rate. The sample cast in water did not present any such crystals, confirming that crystals were not present in the glass melt at 1350°C but were formed during cooling.

Results obtained from rheology experiments (Figure 7) indicate the temperature at which the glass melt contains a significant amount of crystals. Above 1250°C, glass melts containing up to 15 wt% NiO are still Newtonian. Thus, above 1250°C one can expect a very small number of crystals in the melt. The appearance of crystals in high amounts is estimated to occur at between 1100°C and 1200°C, depending on the NiO content of the glass.

4.2. Crystallization path in as-quenched and slowly-cooled samples

4.2.1. As-quenched glass (CP samples)

As-quenched samples of glasses containing 13.5 and 15 wt% NiO showed the same crystalline pattern. A crystalline primary phase NiO was formed, and served as the nucleation point for a secondary Ni-containing phase, enriched in aluminium and silicon. The nature of this secondary phase could not be identified in as-quenched samples due to the sub-micron size and the low number of the crystals. Additionally, the crystal distribution was non-homogeneous. The NiO crystals and crystals growing out of it could only be observed at the sample surface and not in the bulk.

4.2.2. Slowly-cooled glass (RLT samples)

Crystalline phases in the CP and RLT samples were different, showing the influence of cooling rate on crystallization. The NiO crystals (primary phase) present in CP samples were no longer present in RLT samples of glass containing up to 10 wt% NiO. In these samples, the $\text{Ni}_2\text{Al}(\text{BO}_3)\text{O}_2$ phase and the NiAl_2O_4 - Ni_2SiO_4 spinel solid solution were present in small amounts and the crystals were only located at the glass surface. From the analysis of EH Ni-6.5 RLT and Ni-7.5 RLT glasses, it appears that the spinel solid solution serves as a nucleation point for the $\text{Ni}_2\text{Al}(\text{BO}_3)\text{O}_2$ crystals (Figure 18 and Figure 19 in the Appendix). For large crystals, the spinel solid solution tended to be slightly enriched in Ni through the formation of Ni_2SiO_4 , richer in Ni than NiAl_2O_4 , until it was rich enough to form $\text{Ni}_2\text{Al}(\text{BO}_3)\text{O}_2$. It also resulted in a local Si enrichment of the residual glass in the vicinity of the crystals.

The EH Ni-10 RLT glass presented the same crystalline phases but in greater quantity, and more importantly spread throughout the glass and no longer located only at the sample surface (Figure 12).

Above 10 wt% NiO, new types of crystals appeared, as shown by the results obtained for EH Ni-15 RLT glass sample. This sample not only presented spinel solid solution and $\text{Ni}_2\text{Al}(\text{BO}_3)\text{O}_2$ phases, as a NiO crystalline primary phase and a lanthanum-based phase were also found. Because of the formation of very large amounts of crystalline phase, the residual glass composition was impacted, with the main impact coming from an aluminium depletion in the glass matrix caused by the formation of NiAl_2O_4 and $\text{Ni}_2\text{Al}(\text{BO}_3)\text{O}_2$ crystalline phases. Local aluminium depletion was associated with a relative enrichment in sodium, lithium and calcium, in turn impacting lanthanum solubility. According to literature, lanthanum solubility is strongly dependant on the Rp ratio (1) in aluminoborosilicates^[9, 10]. The results obtained for EH Ni-15 RLT sample show a local formation of a lanthanum-based phase around large crystals rich in aluminium. When aluminium depletion was increased further, phase separation between a silicate phase and a lanthanum rich boron phase occurred, as depicted in Figure 20 and explained by Lij at al.^[17].

4.3. NiO structural properties in peraluminous glass

Experimental results from this study enable assumption to be made about the NiO structural role in peraluminous glass. The glass samples were yellow brown below 5 wt% NiO and became dark brown above 5 wt%. These colours are typical of glasses with a mix of Ni^{2+} [4] and Ni^{2+} [5]^[1, 3, 4]. Even though Juze et al.^[6] identified yellow brown glasses as containing Ni^{2+} [6], more recent studies by Galois et al. showed that the peaks that were thought to represent Ni^{2+} [6] are actually a mix of either Ni^{2+} [4] and

$\text{Ni}^{2+}[5]$, or $\text{Ni}^{2+}[5]$ alone^[1,2]. Moreover, the presence of $\text{Ni}^{2+}[6]$ would turn the glass blue or purple^[3,4]. In addition, UV-visible absorption spectra of the samples used in this work are extremely similar to those obtained by Moritomo et al.^[3], Qiu et al.^[4] and Galois and al.^[14] who only attributed peaks to $\text{Ni}^{2+}[4]$ and $\text{Ni}^{2+}[5]$. Another argument in favour of $\text{Ni}^{2+}[4]$ and $\text{Ni}^{2+}[5]$ rather than of $\text{Ni}^{2+}[6]$ coordination is related to the stability of lanthanum-containing peraluminous glasses. The ability of peraluminous glass to incorporate high amounts of rare earths comes from the specific role rare earths play in the stabilization of such glasses^[10]. In peraluminous glasses, rare earth atoms compensate AlO_4^- units of network former Al^{3+} cations. This charge compensation helps for the glass stability. Because this role can also be assumed by alkaline and alkaline earth cations, the addition of such cations to peraluminous glass reduces the rare earth incorporation limit. This is the reason why there is a strong relationship between the Rp ratio (1) and the rare earth incorporation limit, as shown by Lij et al.^[16]. If we assume a 6-fold coordination for Ni^{2+} , $\text{Ni}^{2+}[6]$ could play a role similar to Ca^{2+} , and adding NiO to the glass composition would increase the Rp ratio and therefore strongly decrease lanthanum solubility. Quantitatively, adding 5 wt% NiO would increase the Rp ratio from 0.31 to 0.45 (Figure 9). According to Lij et al., such an Rp variation would bring La_2O_3 solubility from 40 wt% to less than 20 wt%. This reinforces our hypothesis that Ni^{2+} cations, which do not cause lanthanum to re-crystallize as they are added to the glass, do not play a similar role to Na^+ , Li^+ or Ca^{2+} cations. In other words, Ni^{2+} should not be in a 6-fold coordination and is not likely to be a network modifier or a charge compensator in peraluminous glass. Therefore, nickel could be expected to have a similar structural role in peraluminous and peralkaline glasses. In the latter, NiO has been considered as an intermediate oxide in the literature, according to the bond-strength criteria theory in glass forming ability^[18-20]. Experimental results from the work described here show that NiO addition to the glass composition leads to a strong viscosity decrease, as shown in Figure 6. Since NiO is not thought to act as a network modifier, one can assume that NiO acts as a weak network former in the glass compositions of interest. This is also in agreement with the fact that NiO addition does not lead to a Tg decrease, as shown from the DTA measurements (Figure 8).

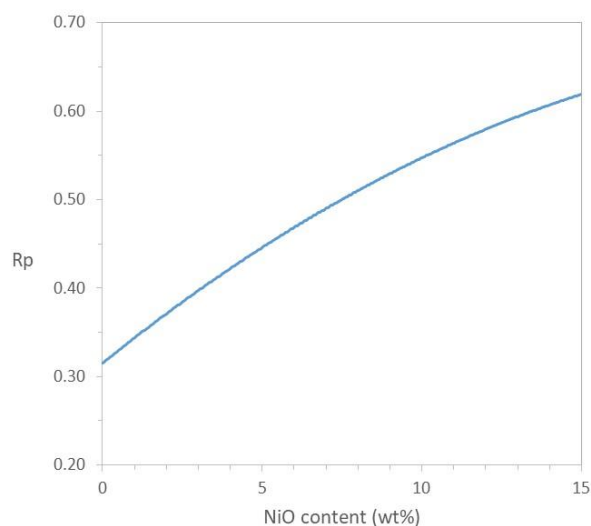


Figure 9: Rp ratio evolution with NiO content, considering Ni^{2+} plays a structural role similar to Ca^{2+}

5. Conclusion

The NiO incorporation limit in peraluminous glasses is strongly dependant on the thermal history of the glass. This incorporation limit is higher for as-quenched glass samples, which are stabilized at higher temperatures, than for slowly-cooled glasses. NiO addition to peraluminous glass leads to a strong decrease of the glass melt viscosity, without decreasing the glass transition temperature. Based on the

results of this study, we suggest the hypothesis that Ni²⁺ is present in both 4-fold and 5-fold coordination, and plays a weak network former role in peraluminous glass, similar to its role in peralkaline glass.

6. Acknowledgement

The authors would like to thank our Orano and EDF partners for financial support.

7. References

- [1] L. Galois, G. Calas, Structural Environment of Nickel in Silicate Glass/Melt Systems: Part 1: Spectroscopic Determination of Coordination States, *Geochimica and Cosmochimica Acta*, vol.57, 3613-3626, 1993
- [2] L. Galois, G. Calas, Structural Environment of Nickel in silicate glass/melt systems: Part 2. Geochemical Implications, *Geochimica et Cosmochimica Acta*, vol.57, pp.3627-3633, 1993.
- [3] Morimoto. S. Luminescence characteristics of Ni²⁺ ion-doped Glasses and Glass-Ceramics in Relation to its Coordination Number, *Journal Of Solids Mechanics and Materials Engineering*, Vol. 1, N°4, 2007
- [4] Qiu. J. Transparent Ni²⁺-doped silicate glass ceramics for broadband near-infrared emission, *Optical Materials*, 30 1900–1904, 2008
- [5] Schultz. P. C. Optical Absorption of the Transition Elements in Vitreous Silica, *Research and Development Laboratories, Corning Glass Works, Corning, New York* 14830
- [6] Juza. R. Color Centers in Alkali Borate Glasses Containing Cobalt, Nickel, or Copper, *Angew. Chem. Internat. Ed.* 1 Vol. 5 (1966)
- [7] Degeng. D et al. Broadband infrared luminescence of Ni²⁺-doped silicate glass–ceramics containing lithium aluminate spinel nanocrystals, *Journal of Non Crystalline Solids* 357 (2011)
- [8] Bamford, C. R. (1962). "The application of the ligand field theory to coloured glasses." *Phys. Chem. Glasses* 3(6): 189-202.
- [9] E. Gasnier, *Etude Structurale et Propriétés de Verres Peralumineux de Conditionnement des Produits de Fission et Actinides Mineurs*, Thèse Université d'Orléans, Soutenue le 18/10/2013.
- [10] V. Piovesan, *Relations Composition-Structure-Propriétés des Verres Peralumineux pour le Conditionnement des Déchets Nucléaires*, Université d'Orléans, Soutenue le 30/11/2016
- [11] V. Piovesan, I. Bardez-Giboire, D. Perret, V. Montouillout, N. Pellerin, Effect of composition on peraluminous glass properties: An application to HLW containment, *Journal of Nuclear Materials*, 483, 90-101, 2017
- [12] M. A. Villegas, J. Alarcon, Crystallization and microstructural development of nickel-containing aluminosilicate glasses with cordierite stoichiometry, *Journal of Non-Crystalline Solids* 292, 70-79, 2001
- [13] Akaogi, M., S.-I Akimoto, K. Horioka, K. -I. Takahashi and H. Horiuchi, "The System NiAl₂O₄-Ni₂SiO₄ at High Pressures and Temperatures: Spinelloids with Spinel-Related Structures' *Journal of Solid State Chemistry*, 44, 257-267 (1992).

- [14] R. Kado, L. Galois et al. Structural significance of nickel sites in aluminosilicate glasses, *Journal of Non-Crystalline Solids* 539, 2020.
- [15] J. D. MacKenzie, *Modern Aspects of the Vitreous State*, Butterworths & Co Ltd, London (1960)
- [16] H. Scholze, *Glass: Nature, Structure, and Properties*, Springer New York (1991)
- [17] H. Liyu, J-D. Vienna, M-J. Schweiger, and J-V. Crum, *Ceram. Trans.* 87, *Environmental Issues and Waste Management Technologies in the Ceramic and Nuclear Industries* 189 (1) (1998).
- [18] Boubata N. et al., *Bull. Mater. Sci.*, 36 (3), 457-460, 2013
- [19] Paul A., *Chemistry of Glasses*, First published by Chapman and Hall Ltd, London, 1982
- [20] Rawson, H., *Proc. IV Internat. Congr. on Glass*, Imprimerie Chaix, Paris, 1956

Appendix

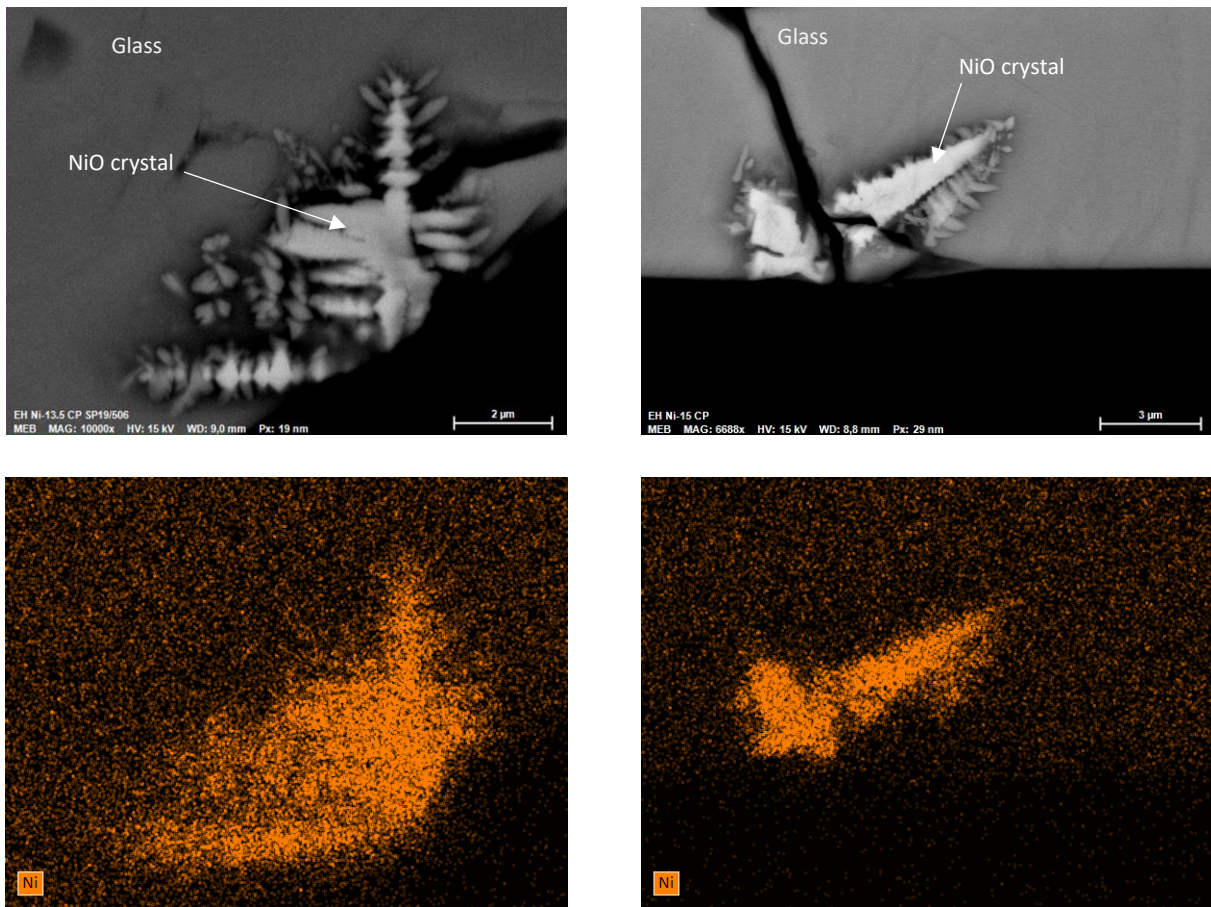


Figure 10: SEM images (top) and WDS cartography (bottom) of as-quenched samples containing 13.5 wt% NiO (left) and 15 wt% NiO (right) showing the appearance of first crystals at the sample surface

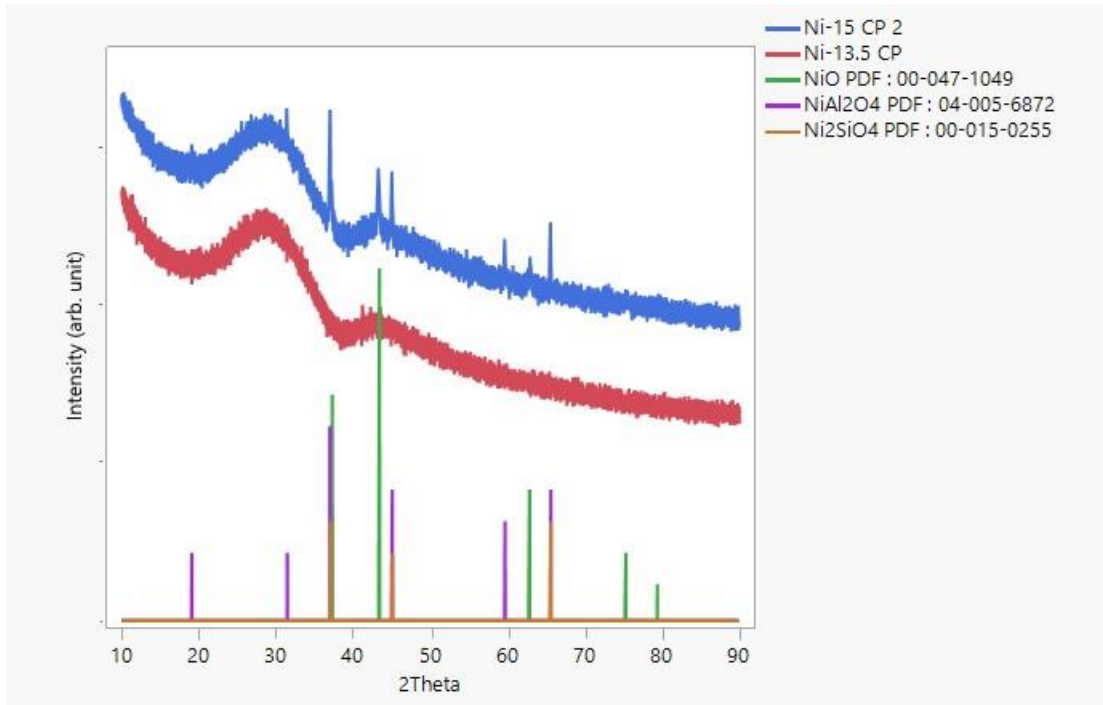


Figure 11: XRD patterns of as-quenched samples containing 13.5 wt% and 15 wt% NiO with peak indexation

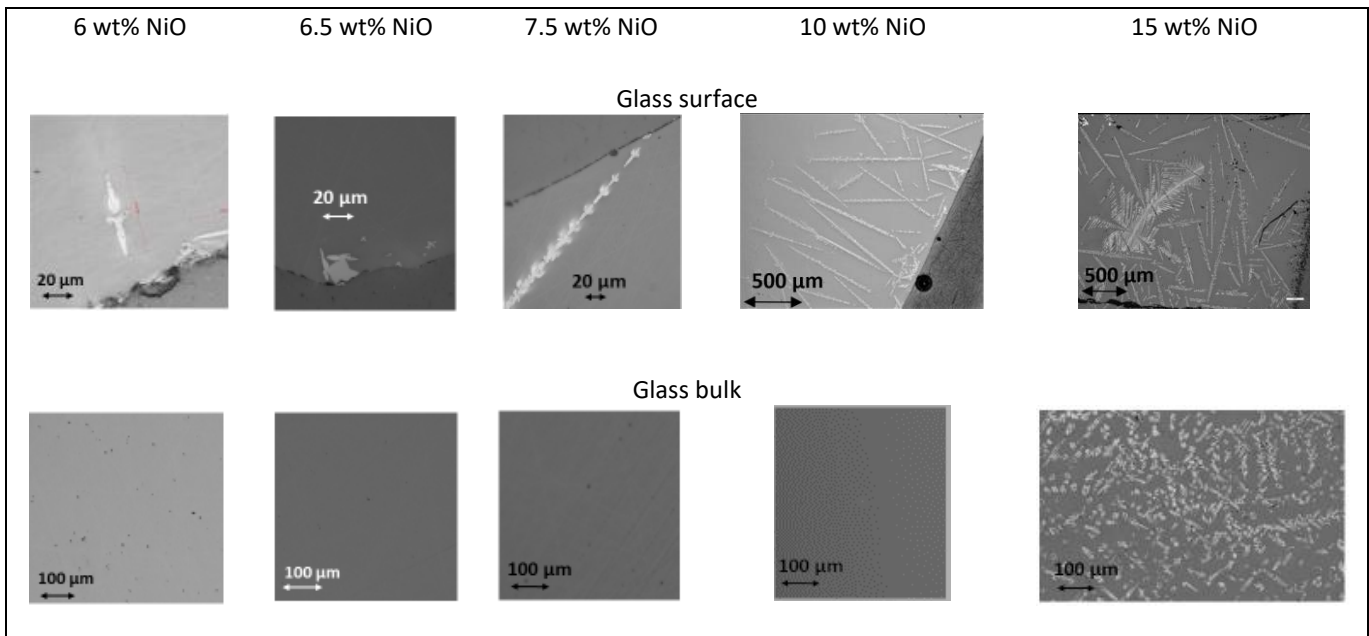


Figure 12: Optical microscopy images of the surface and bulk evolution of slowly-cooled glass samples with different NiO amounts

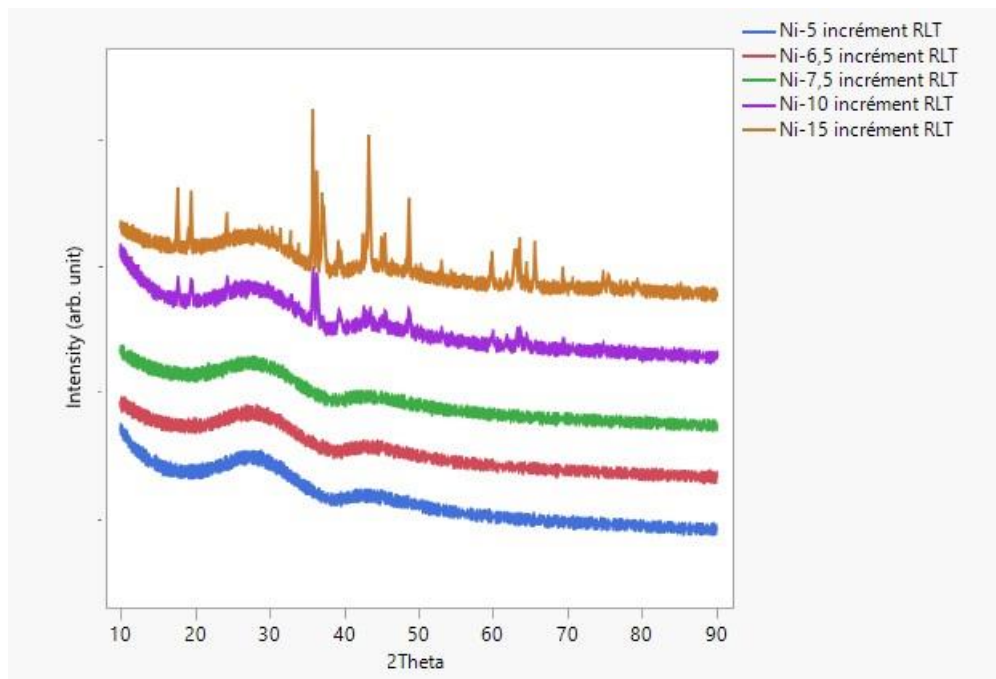


Figure 13: XRD patterns of slowly-cooled samples containing 5 wt% to 15 wt% NiO

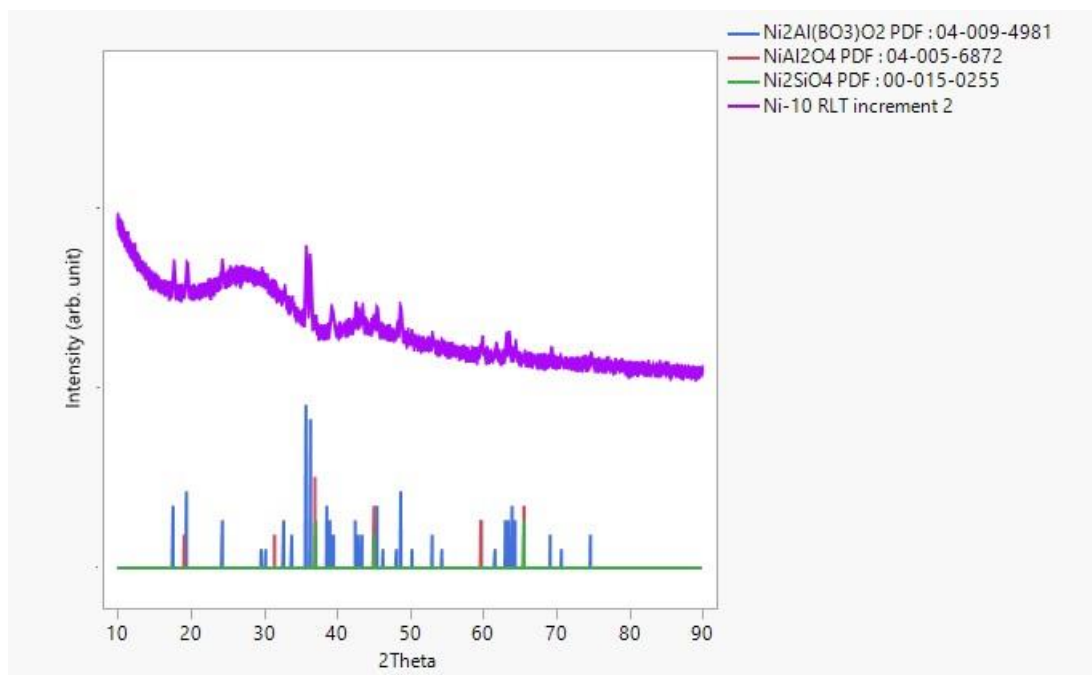


Figure 14: XRD patterns of slowly-cooled sample containing 10 wt% NiO with peak indexation

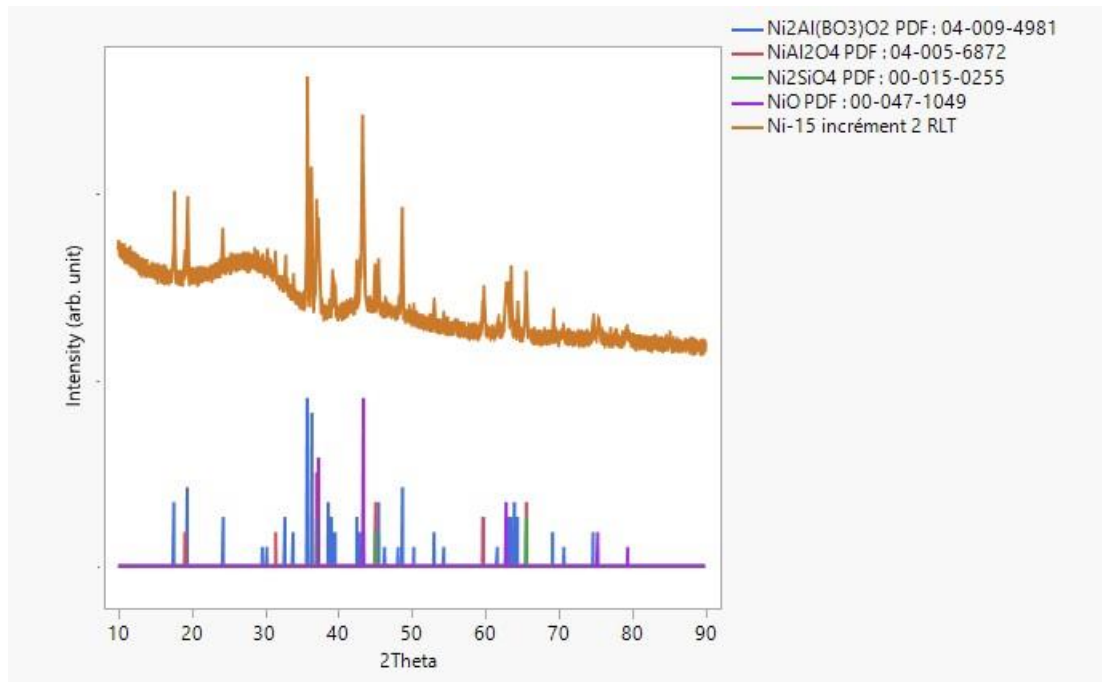


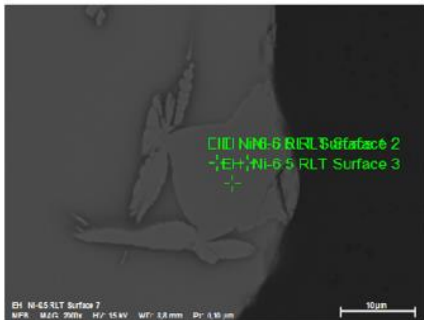
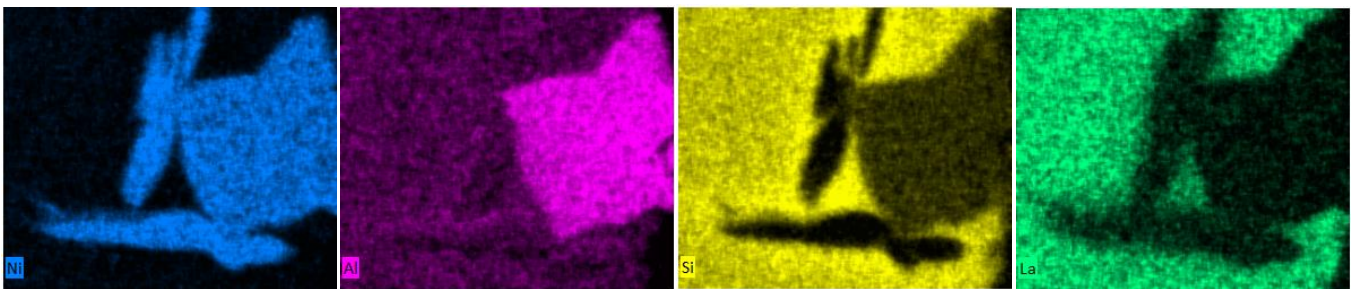
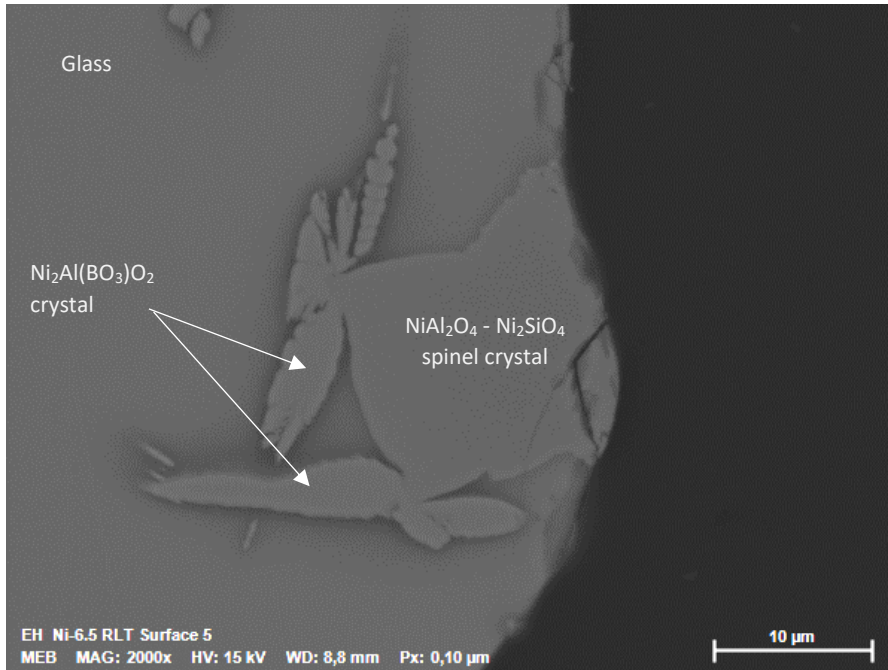
Figure 15: XRD patterns of slowly-cooled sample containing 15 wt% NiO with peak indexation

Point	B2O3 (wt%)	Al2O3 (wt%)	SiO2 (wt%)	NiO (wt%)	La2O3 (wt%)	Total
1	12.3	27.4	0.1	61.7	0.3	101.8
2	12.4	27.3	0.2	61.3	0.3	101.4
3	12.7	27.3	0.3	61.1	0.1	101.5
4	12.1	27.1	0.1	62.1	0.3	101.7
5	12.3	27.5	0.2	61.6	0.2	101.7
6	12.2	27.2	0.3	61.9	0.1	101.7
mean	12.3	27.3	0.2	61.6	0.2	101.6
std err	0.2	0.1	0.1	0.4	0.1	0.2
Ni2Al(BO3)O2 theor. compo.	14.8	21.7		63.5		100.0

Figure 16: Microprobe analysis of Ni₂Al(BO₃)O₂ crystal in slowly-cooled sample containing 15 wt% NiO (wt% of oxides)

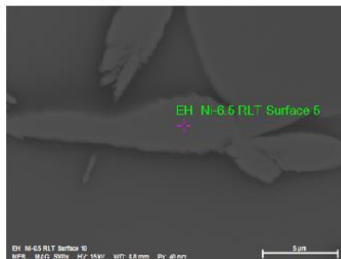
Point	B (at%)	Al (at%)	Si (at%)	Ni (at%)	La (at%)	O (at%)	Total
1	9.1	13.8	0.1	21.2	0.1	55.8	100.0
2	9.2	13.8	0.1	21.1	0.0	55.8	100.0
3	9.4	13.7	0.1	21.0	0.0	55.8	100.1
4	9.0	13.8	0.0	21.5	0.0	55.7	100.1
5	9.1	13.9	0.1	21.2	0.0	55.8	100.0
6	9.1	13.7	0.1	21.4	0.0	55.8	100.1
mean	9.1	13.8	0.1	21.2	0.0	55.8	100.0
std err	0.1	0.0	0.0	0.2	0.0	0.0	0.0
Ni ₂ Al(BO ₃)O ₂ theor. compo.	11.1	11.1		22.2		55.6	100.0

Figure 17: Microprobe analysis of Ni₂Al(BO₃)O₂ crystal in slowly-cooled sample containing 15 wt% NiO (at%)



Spectrum	oxygène	Al2O3	SiO2	NiO	Sum
EH Ni-6.5 RLT Surface 1	0,00	40,35	10,41	51,32	102,08
EH Ni-6.5 RLT Surface 2	0,00	41,29	10,08	51,15	102,52
EH Ni-6.5 RLT Surface 3	0,00	40,46	10,36	51,07	101,88
Mean	0,00	40,70	10,28	51,18	102,16
Sigma	0,00	0,52	0,18	0,13	0,33
SigmaMean	0,00	0,30	0,10	0,07	0,19

	NiAl2O4 x	Ni2SiO4 (1-x)	spinel solid solution
wt% NiO	42.3	71.3	52.4
wt% Al2O3	57.7		37.5
wt% SiO2		28.7	10.0
	100.0	100.0	100.0



Spectrum	oxygène	Al2O3	SiO2	NiO	La2O3	Sum
EH Ni-6.5 RLT Surface 4	0,00	23,41	3,17	62,08	2,52	91,18
EH Ni-6.5 RLT Surface 5	0,00	23,13	2,63	62,10	2,71	90,57

$NiO/(NiO+Al2O3) = 0.73$	
	Ni2Al(BO3)O2
%NiO	63.5%
%Al2O3	21.7%
%B2O3	14.8%
	100.0%
$NiO/(NiO+Al2O3) = 0.75$	

Figure 18 : Crystalline phases identification under SEM/EDS in slowly-cooled sample containing 6.5 wt% NiO

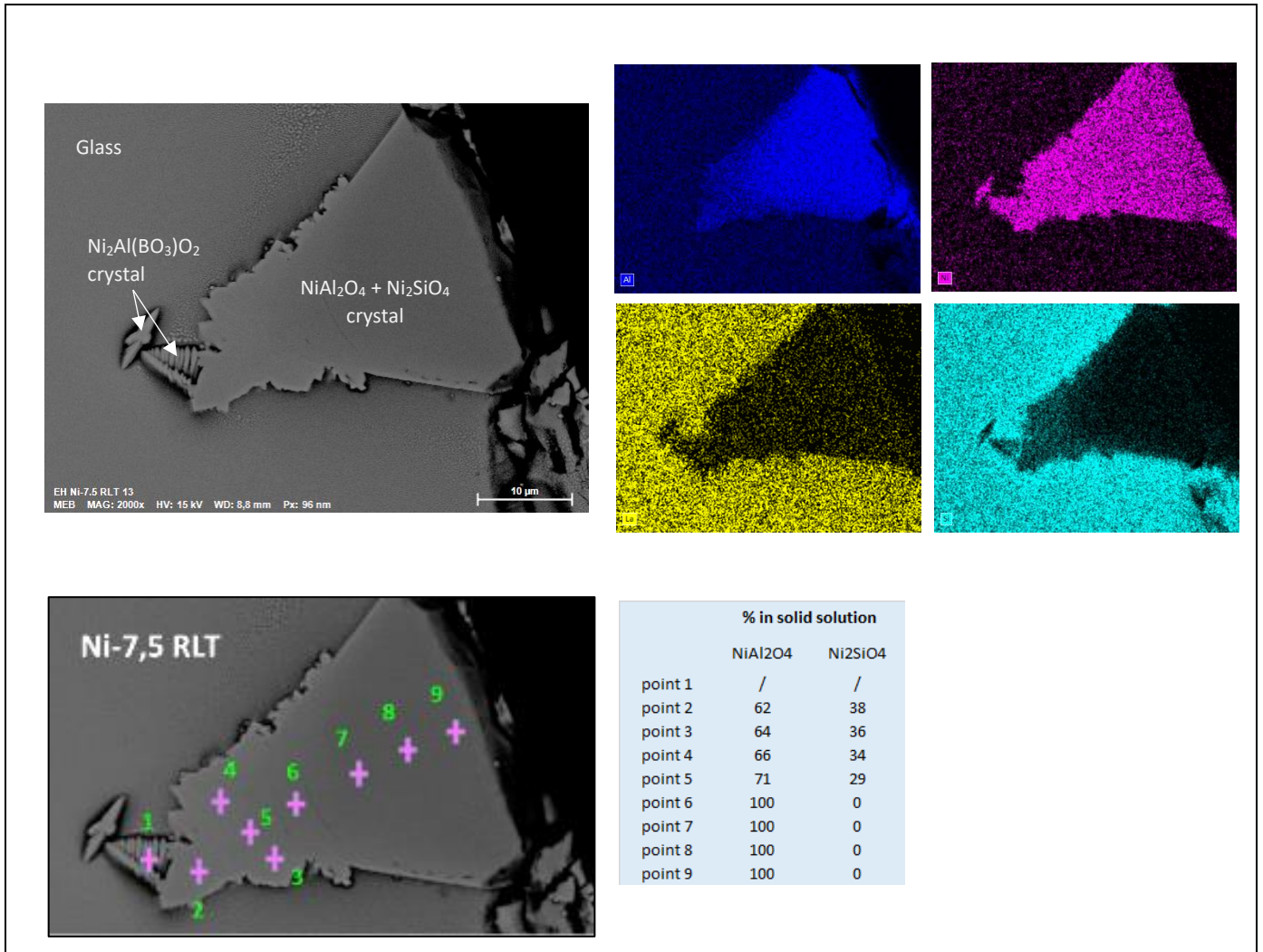


Figure 19: Observation of spinel solid solution under SEM/EDS in slowly-cooled sample containing 7.5 wt% NiO

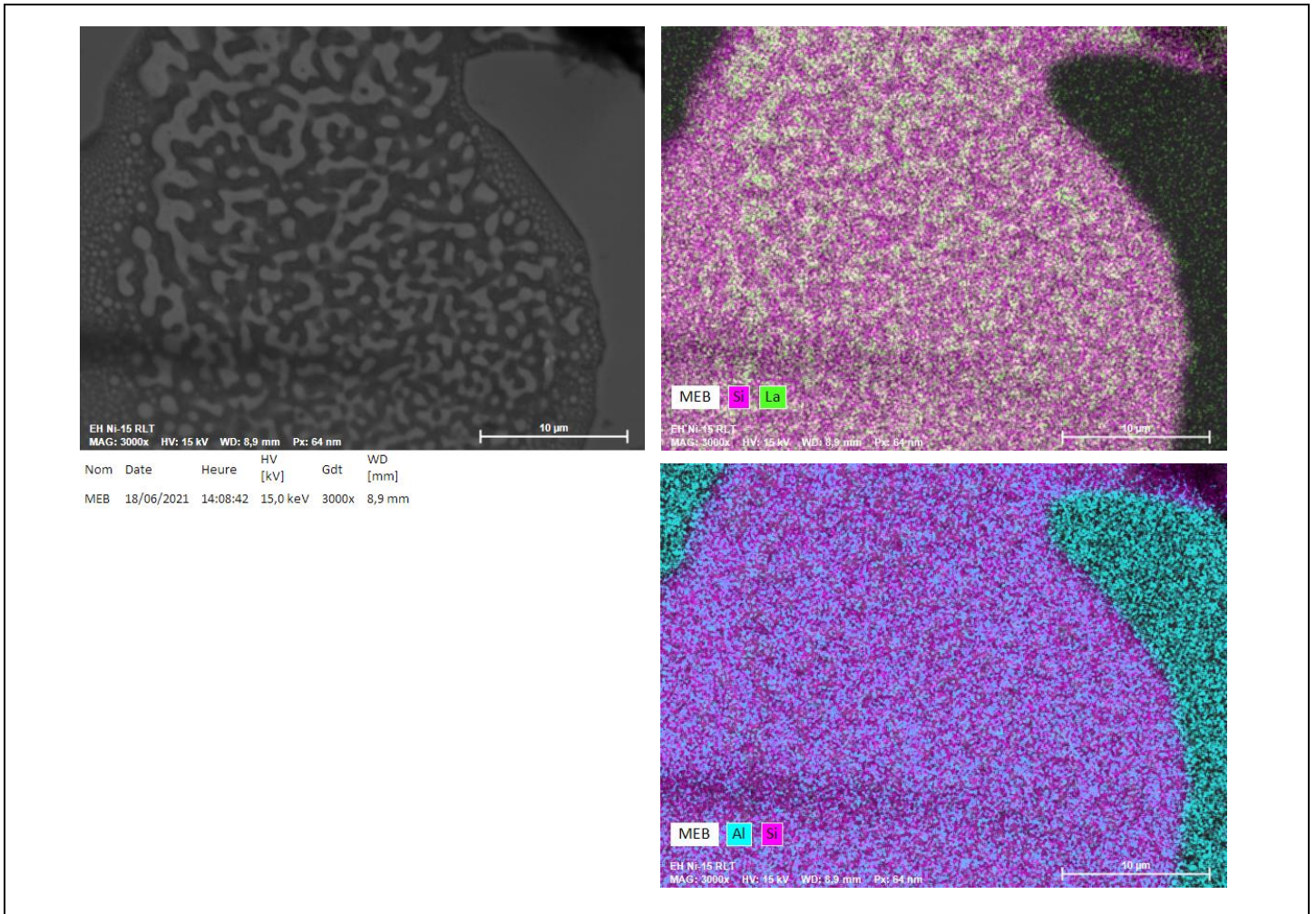


Figure 20: Observation of local phase separation under SEM/EDS in slowly-cooled sample containing 15 wt% NiO

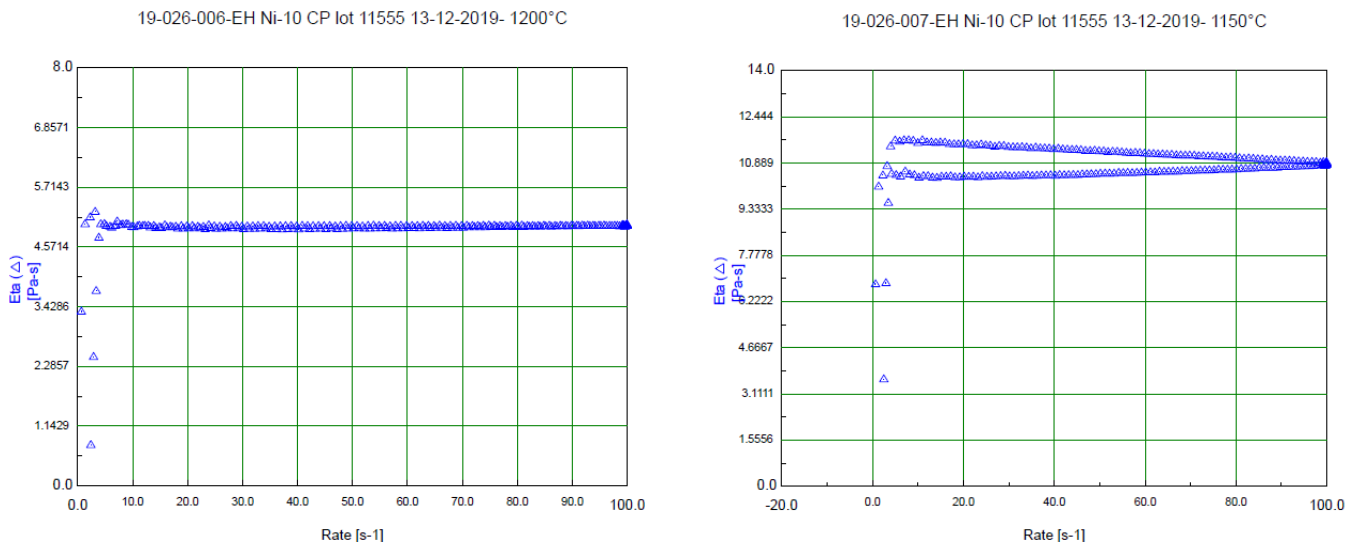


Figure 21: Eta vs Rate experimental plots showing the Newtonian behavior loss between 1200°C and 1150°C in glass sample containing 10 wt% NiO